nature chemistry

ARTICLES

https://doi.org/10.1038/s41557-019-0280-3

Enhanced reactivity of fluorine with *para*-hydrogen in cold interstellar clouds by resonance-induced quantum tunnelling

Tiangang Yang[1,8], Long Huang[1,2,8], Chunlei Xiao[1,8], Jun Chen[1], Tao Wang[3], Dongxu Dai[1], Francois Lique[4], Millard H. Alexander[5*], Zhigang Sun[1*], Dong H. Zhang[1], Xueming Yang[1,3*] and Daniel M. Neumark[6,7*]

Chemical reactions are important in the evolution of low-temperature interstellar clouds, where the quantum tunnelling effect becomes significant. The $F+para\text{-}H_2\rightarrow HF+H$ reaction, which has a significant barrier of 1.8 kcal mol^{-1}, is an important source of HF in interstellar clouds; however, the dynamics of this quantum-tunnelling-induced reactivity at low temperature is unknown. Here, we show that this quantum tunnelling is caused by a post-barrier resonance state. Quantum-state-resolved crossed-beam scattering measurements reveal that this resonance state has a collision energy of ~5 meV and a lifetime of ~80 fs, which are in excellent agreement with a recent anion photoelectron spectroscopic study. Accurate quantum reactive scattering calculations on the new iCSZ-LWAL potential energy surfaces provides a detailed explanation of the experimental results. The reaction rate for this system was also theoretically determined accurately at temperatures as low as 1 K.

In the classical picture, a chemical reaction with an energy barrier can only happen at collision energies higher than the barrier. However, at energies below the reaction barrier, chemical reactions through quantum tunnelling can play a significant role in many chemical and biological processes[1–3]. Quantum tunnelling is especially important in low-temperature environments such as the interstellar medium[4,5]. Thus, understanding quantum tunnelling in chemical reactions is of general interest and of fundamental importance to interstellar chemistry.

The $F+H_2\rightarrow HF+H$ reaction has been a benchmark system for the study of chemical reaction dynamics in recent decades[6]. Its importance in the interstellar medium has also been recognized[7,8]. HF was first discovered in the interstellar cloud (ISC) in 1997, and recent observations by the Herschel Space Observatory found that the existence of HF is ubiquitous in the universe[8–10]. It has been used to trace key properties of the ISC, such as hydrogen column density. This discovery has generated renewed interest in the benchmark $F+H_2$ reaction in the low-temperature region, because it is the sole source of the observed HF in low-temperature ISC[10]. Clearly, the reaction rate of this system at temperatures close to absolute zero is very important for modelling ISC chemistry. It is already known that for reactions such as the $S(^1D)+H_2$ reaction[11–13], which has no reaction barrier, the reaction rate at very low temperatures is usually very large. However, the $F+H_2$ reaction is known to have a significant reaction barrier ($E_a\approx 1.8$ kcal mol^{-1} or 78 meV), so its reaction rate should be negligibly small at low temperatures around $T=10$ K ($E_T=0.86$ meV), which are quite typical in the ISC, even when the normal quantum tunnelling effect below the reaction barrier is taken into consideration. A recent rate measurement of the $F+H_2$ reaction at temperature as low as 12 K showed pronounced chemical reactivity of this reaction at an extremely low temperature[14]. This rather surprising result raises an intriguing question: what is the exact mechanism of the enhanced $F+H_2$ reactivity at extremely low temperatures that produces HF in the low-temperature ISC?

As one of the most important prototype reactions for the study of reaction dynamics and the development of the concept of reaction resonances, the $F+H_2$ reaction (and its isotopic reactions) has been investigated extensively in recent decades using various advanced experimental methods and accurate quantum dynamics theories[15–19]. The existence of a reaction resonance in the $F+H_2$ reaction was predicted in 1973 in refs. [20] and [21]. In 1985, a forward scattering peak for the $HF(v'=3)$ product was observed in a crossed-beam scattering experiment (which was regarded as a signature of reaction resonances) from this seemingly direct abstract reaction[22,23]. Both quasi-classical trajectory[24] and quantum dynamics calculations[25] on the Stark–Werner potential energy surface (SW-PES)[26] show a forward scattering peak for $HF(v'=3)$, with the quasi-classical trajectory results smaller than the experiment. In the past two decades, reaction resonances in the $F+HD$ system have been investigated and characterized in great detail[27–29]. Even though reaction resonances in the $F+H_2\rightarrow HF+H$ reaction have also been investigated quite extensively[30–33], the lowest resonance state in the reaction has not been characterized directly in a crossed-molecular-beam study, and its role in the chemical reactivity at the cold interstellar temperature has not been clearly understood. This is largely due to the

---

[1]State Key Laboratory of Molecular Reaction Dynamics, Dalian Institute of Chemical Physics, Chinese Academy of Sciences, Dalian, Liaoning, China. [2]University of Chinese Academy of Sciences, Beijing, China. [3]Department of Chemistry, College of Science, Southern University of Science and Technology, Shenzhen, China. [4]Laboratoire Ondes et Milieux Complexes, CNRS-Université Le Havre Normandie and Institut Universitaire de France, Le Havre, France. [5]Department of Chemistry and Biochemistry and Institute for Physical Sciences and Technology, University of Maryland, College Park, MD, USA. [6]Department of Chemistry, University of California at Berkeley, Berkeley, CA, USA. [7]Chemical Sciences Division, Lawrence Berkeley National Laboratory, Berkeley, CA, USA. [8]These authors contributed equally: Tiangang Yang, Long Huang, Chunlei Xiao. *e-mail: mha@umd.edu; zsun@dicp.ac.cn; xmyang@dicp.ac.cn; dneumark@berkeley.edu

difficulties in studying the dynamics of this reaction at very low collision energy using the crossed-molecular-beam method.

To understand the role of resonances in the $F + H_2$ reaction at the cold interstellar temperature, we carried out a high-resolution crossed-beam scattering study on the $F + H_2 \rightarrow HF + H$ reaction at a collision energy as low as 1.21 meV, using the H-atom Rydberg tagging time-of-flight (TOF) technique[34]. Quantum-state-specific backward scattering spectroscopy (QSSBSS), which essentially is the collision-energy-dependent differential cross-sections (DCSs) for a specific product quantum state in the backward scattering direction, was measured in the very low collision energy region, in addition to obtaining full-dimensional DCSs at three collision energies. The present results are also compared with recent results from a high-resolution negative-ion photoelectron spectroscopic study[31] and accurate quantum dynamics calculations in an effort to understand the nature of the $F + H_2$ reactivity at very low temperature. Using a combination of the QSSBSS of the crossed molecular beam scattering technique and negative ion photoelectron spectroscopic technique enables us to obtain a unique perspective on the transition-state resonance. As we show in the following sections, the experimental results agree with each other well, which demonstrates the power of these two state-of-the-art experimental methods for characterizing a transition state.

Results and discussion

Crossed molecular beam and anion photoelectron spectroscopy experiment. The crossed molecular beam apparatus used in this work was specially modified so that a reactive scattering experiment on the title reaction at very low collision energy could be carried out. Using this apparatus, TOF spectra were measured for the H-atom product in the backward scattering direction from the $F(^2P_{3/2}) + H_2(v=0, j=0) \rightarrow HF(v', j') + H$ reaction in the low collision energy region. Three typical TOF spectra are shown in Fig. 1, with the lowest collision energy at 1.21 meV. From these spectra, it is clear that the HF products are predominantly populated in the $v' = 2$ state in the low collision energy region.

The QSSBSS has been demonstrated to be a powerful method to probe the isolated quantum resonances in several benchmark chemical reactions[27,35,36], and can effectively minimize partial waves averaging in reactive scattering experiments. Here, we measured the QSSBSS for the $HF(v'=2)$ product from the $F + H_2(v=0, j=0)$ reaction for collision energies between 1.21 and 35 meV, in an effort to determine accurately the energy of the reaction resonance state in the low collision energy region (Fig. 2a). A peak at ~5 meV is clearly observed in the QSSBSS, which can be assigned to the lowest resonance state of the $F + H_2 \rightarrow HF + H$ reaction. This peak can be fitted very well using a Lorentzian profile with a full-width at half-maximum of ~5 meV, which corresponds to a lifetime of ~80 fs for this resonance state. The energy of the lowest resonance state was determined to be 4.9 ± 0.5 meV. The feature at a collision energy of ~20 meV is related to the first excited resonance state of this reaction, but mixed with signals from the direct reaction via regular quantum tunnelling through the energy barrier, thus making the resonance feature in the QSSBSS not as clear as the lowest resonance state. In addition to the QSSBSS measurement, the full DCSs at collision energies of 1.56, 6.93 and 9.97 meV were also experimentally measured and are shown in Fig. 3. As pointed out in the Methods, the uncertainty of collision energy in this experiment is ~10%, that is, 0.5 meV at a collision energy of 5 meV.

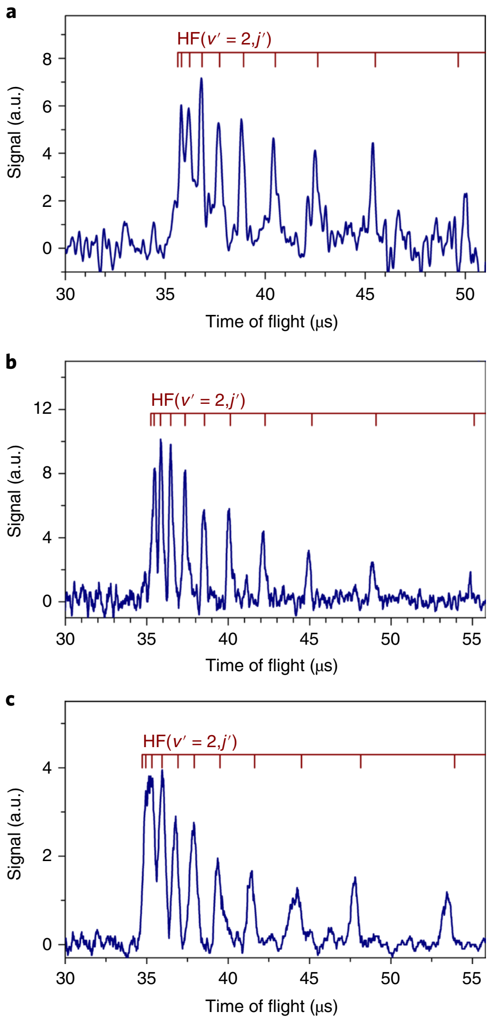

Fig. 1 | TOF spectra of the H-atom product from the $F + H_2(v=0, j=0) \rightarrow HF(v') + H$ reaction at 180° in the centre-of-mass frame. a–c, TOF spectra for collision energies of 1.21 meV (**a**), 3.25 meV (**b**) and 9.10 meV (**c**). The product rotational state-resolved information is clearly observed.

Anion photoelectron spectroscopy has been used to probe the transition-state resonances in the $F + H_2$ reaction[37]. Recently, the high-resolution anion photoelectron spectrum for FH_2^- has been measured using the cryo-SEVI (slow-electron velocity-map imaging with cryogenic ion cooling) technique, a high-resolution photoelectron spectroscopy method, to detect the transition-state resonances of the $F + H_2$ reaction[31]. Figure 2b presents a plot of the photoelectron spectrum of FH_2^-, with the collision energy on the x axis, which can be compared directly with the QSSBSS results in Fig. 2a. Conversion of the photoelectron energy to the collision energy is carried out using the relationship described in Supplementary Section A. The main resonance peak (peak A) position was determined to be at 5.4 meV in the cryo-SEVI spectrum in terms of the collision energy in this experiment. Here, we use the most recent theoretical value for the dissociation energy of FH_2^-, $D_0(FH_2^-) = 0.2028$ eV (ref. [38]), obtained using a highly accurate ab initio method, and the electronic affinity energy of the F atom from experiment, EA(F) = 3.4012 eV (ref. [39]), to rescale the cryo-SEVI spectrum for comparison with the QSSBSS result (Supplementary Fig. 1). The resonance state energy in the rescaled cryo-SEVI spectrum is in excellent agreement with the resonance energy (4.9 ± 0.5 meV) obtained in the QSSBSS measurements (Fig. 2a). The small disagreement between the two numbers could come from the uncertainty of the theoretical value of $D_0(FH_2^-)$ and the experimental measurement errors. Thus, the position of the lowest resonance state in terms of collision energy is accurately determined to within 0.5 meV from these two accurate experimental methods, which allows us to benchmark the resonance picture of the $F + H_2$ reaction with high accuracy. Furthermore, the width of

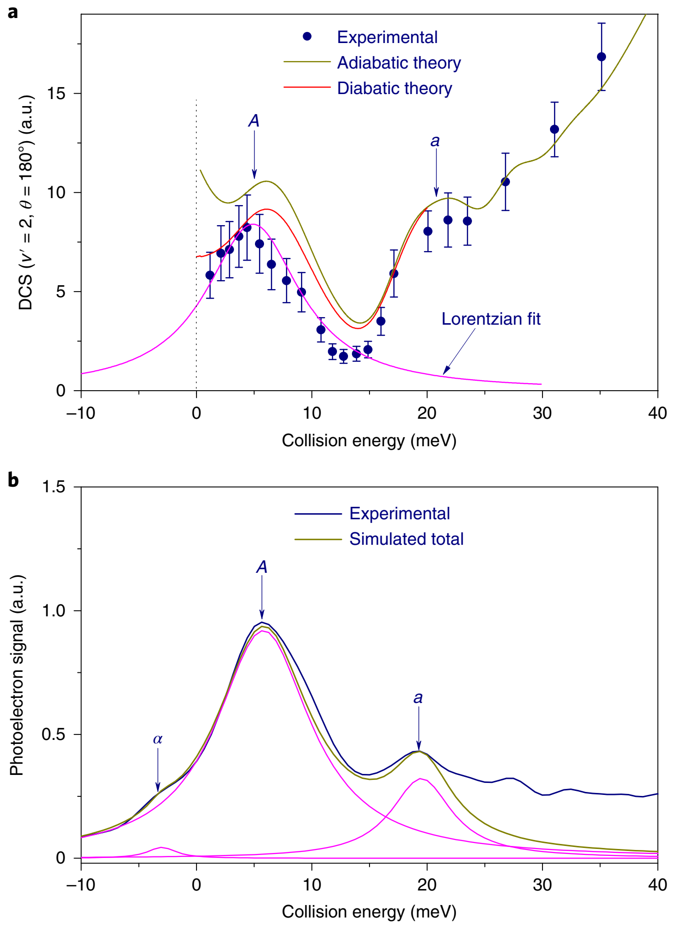

Fig. 2 | QSSBSS of the $F + H_2(v = 0, j = 0) \rightarrow HF(v' = 2) + H$ reaction and photodetachment spectra of *p*-FH_2^-. a, Experimental (filled symbols) and theoretical (red and olive lines) QSSBSS for the backward scattering $HF(v' = 2)$ product from the $F + H_2(v = 0, j = 0)$ reaction. The experimental QSSBSS values for $HF(v'' = 2)$ were obtained by averaging the results of 10 repeated measurements for each collision energy, and the corresponding error bar is 1 s.d. of uncertainty. The olive line was calculated using the adiabatic iCSZ PES, and the red line was calculated using the diabatic iCSZ-LWAL PESs. The magenta line is the Lorentzian fit to the lowest peak. **b**, Experimental photodetachment spectra[31] of *p*-FH_2^- with a resolution of ~2–3 meV over a narrow energy window (deep blue line). The magenta lines come from fittings with the Lorentzian function to the three peaks, α (−3.0 meV), *A* (5.4 meV) and *a* (19 meV), which correspond to the van der Waals resonance in the reactant channel, the ground reactive resonance and the first excited reactive resonance state, respectively. The olive line is the total fitting curve. Structures in the QSSBSS and photodetachment spectra agree with each other very well.

this resonance peak in the cryo-SEVI spectrum (Fig. 2b) also agrees very well with that of the corresponding feature in the QSSBSS results (Fig. 2a). The excellent agreement between this experiment and the cryo-SEVI experiment is clearly a great achievement of the two state-of-the-art experimental methods for studying reaction resonances, which have never been so closely compared on the same reaction system.

According to theoretical calculations based on the improved adiabatic ground-state iCSZ PES (see the following subsection), the lowest resonance peak in the QSSBSS can be assigned to the ground resonance state on the vibrationally adiabatic potential (VAP) of $H\cdots HF(v' = 3)$ in the exit channel (post-barrier region) of the $F + H_2$ reaction (Fig. 4). Additionally, the resonance feature at ~20 meV in the cryo-SEVI spectrum (Fig. 2b) is in good agreement with the bump feature in the QSSBSS (Fig. 2a) at roughly the same collision energy. This feature can be assigned to the excited resonance state on the same VAP. In the spectrum of Fig. 2b, there is also a small bump at a collision energy of ~−3 meV in the anion photoelectron spectrum, which can be identified as a quantum state in the van der Waals well at the entrance channel (Fig. 4). This state is certainly below the collision energy zero (from accurate energy characterization in the QSSBSS experiment) and thus should not play a significant role in the $F + H_2$ reaction in the low-temperature interstellar medium.

Mechanism investigation by quantum reaction dynamics theory. To understand the role of the observed resonances in the chemical reactivity of $F + H_2$ in the low-temperature region, an improved adiabatic PES for the ground electronic state based on the CSZ PES[40] was constructed, because the CSZ PES does not provide a sufficiently accurate description of the long-range interaction potential in the reactant channel, which is a crucial part of the surface for determining the reactivity at low temperatures. A total of 6,118 ab initio points at the UCCSD(T)/AVQZ level were applied to the CSZ PES to improve its accuracy in the long-range part of the surface. For a more detailed description of this improved CSZ PES (iCSZ PES) for the ground state, see Supplementary Section B.

Using the time-independent reactive scattering ABC code[41], a converged DCS calculation was carried out on the new adiabatic iCSZ PES using the parameters listed in Supplementary Section D. The calculated QSSBSS for the $HF(v' = 2)$ product is presented in Fig. 2a as the olive line. The agreement between theoretical and experimental results is quite good. A small difference in peak position is clearly seen. In addition, in the lowest collision energy region, the theoretical result seems to go up slightly with the collision energy approaching zero, while the experimental result goes down. To test if this difference is due to the spin–orbit non-adiabatic effect, we carried out time-dependent wavepacket calculations (for details see Supplementary Section C)[42,43], which include the spin–orbit coupling in the reaction, based on the new diabatic PESs (iCSZ-LWAL PESs), which are constructed from the iCSZ PES and the diabatic LWAL PESs[44] (for a detailed description of these new diabatic PESs see Supplementary Section B). The adiabatic ground state of the new diabatic PESs uses the iCSZ PES, but the non-adiabatic couplings and excited surfaces of the new diabatic PESs use those of the LWAL PESs[45]. The QSSBSS data below 20 meV are then calculated using the new diabatic PESs. The calculated QSSBSS for the $HF(v' = 2)$ product is shown in Fig. 2a as the red line; this seems to be in better agreement with the experimental result than the adiabatic calculation based on the iCSZ PES in the low collision energy region. The calculated peak position for the lowest resonance using the diabatic iCSZ-LWAL PESs is ~6.1 meV, which is 1.2 meV off the QSSBSS experimental value and 0.7 meV off the cryo-SEVI result. The calculated peak width is also in very good agreement with both experimental results. This is clearly a remarkable achievement of the theory, which has reached far beyond chemical accuracy (1 kcal mol^{-1}). The high accuracy of the PESs also allows us to analyse how the resonance state would affect chemical reactivity in the very low temperature regime.

The DCSs calculated in the entire scattering angular range (0–360°) using the new diabatic iCSZ-LWAL PESs, which include the spin–orbit non-adiabatic coupling effects, were also compared with the experimentally measured DCSs at collision energies of 1.56, 6.93 and 9.97 meV (Fig. 3). The agreement between experiment and theory is quite good. These results suggest that the new diabatic PESs are highly accurate and the inclusion of the spin–orbit coupling seems to have a non-negligible effect in the reaction dynamics of $F(^2P_{3/2}) + H_2(j = 0)$, especially in the collision-energy-dependent DCS in the very low collision energy regime.

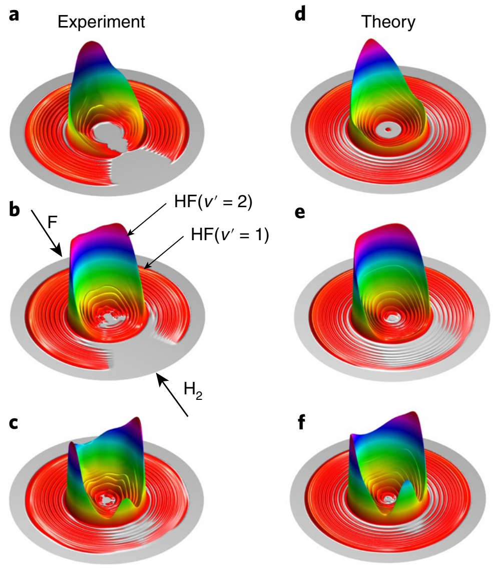

Fig. 3 | Three-dimensional product contour plots as a function of product velocity for the F + H$_2$(v = 0, j = 0) → HF + H reaction. a–f, Product contour versus product velocity plots are shown in the centre-of-mass frame for experimental measurements (**a**–**c**) and theoretical calculations (**d**–**f**) at collision energies of 1.56 meV (**a**,**d**), 6.93 meV (**b**,**e**) and 9.97 meV (**c**,**f**).

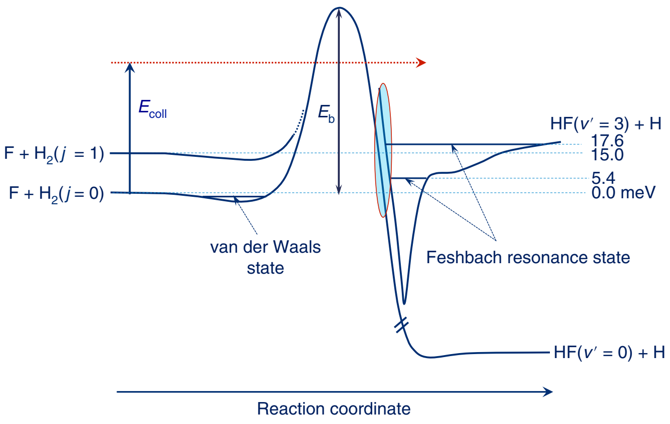

Fig. 4 | Schematic explaining the roles of the two resonances states (003) and (103) in the product channel in the reaction of F + H$_2$(j = 0) and F + H$_2$(j = 1). The ground resonance state in the exit channel (post-barrier) is mainly responsible for the F + H$_2$(j = 0) reaction at very low temperature, while the excited resonance state in the exit channel should play a more important role than the ground resonance state for the F + H$_2$(j = 1) reaction in the very low temperature regime.

To understand how the QSSBSS measurement gives the correct energy position of the resonance state under the average effect of partial waves, the contributions of partial waves to the first peak of the QSSBSS were analysed (Supplementary Figs. 4 and 5). The analysis clearly shows that the partial waves averaging should not shift the peak position of the resonance state in the QSSBSS, and the position of the first resonance peak in the total reaction probabilities for $J = 0$ agrees very well with the position of the first peak in the QSSBSS. This suggests that the QSSBSS resonance peak in the F + p-H$_2$(v = 0, j = 0) reaction only comes from contributions of the lowest few J partial waves. For a better understanding of the nature of the ground resonance state, the corresponding wavefunction is also given in Supplementary Fig. 6. It is seen that there are three nodes along the bond of the diatomic product HF with the resonance state, which is trapped in the adiabatic H…HF(v' = 3) potential energy curve in the exit channel after the reaction barrier, as schematically shown in Fig. 4. Such reaction resonance in the exit channel seems to be quite prevalent in the hydrogen abstraction reaction involving the F atom. In a recent cryo-SEVI study, Feshbach resonances in the post-barrier region were also observed in the reaction of F + CH$_3$OH and its isotopes[46].

Reaction rate constant calculations by quantum dynamics theory. Using the diabatic iCSZ-LWAL PESs, we also investigated the effect of resonance on the reaction rate constants for the F + p-H$_2$ reaction in the low temperature region of interstellar chemistry of interest (see Methods and Supplementary Sections C and D), down to 1 K. In particular, reaction rate constant calculations for the F + p-H$_2$ reaction were carried out by taking out the first resonance state peak in the reaction probability in each partial wave (for details see Supplementary Section H), to see how the ground resonance state affects the reaction rate in the low temperature region. Figure 5 shows the calculated rate constants of the F + p-H$_2$ reaction with and without the ground resonance in the low temperature region. From this figure, we conclude that the F + p-H$_2$ reaction in the low temperature region (below 40 K) is mostly due to the ground reaction resonance state. Similarly, the ICS for the F + p-H$_2$ reaction in the low collision energy region is also predominantly due to the ground resonance state (Supplementary Section E and Supplementary Fig. 2). Obviously, this post-barrier resonance enhanced tunnelling is very different from traditional quantum tunnelling immediately below the reaction barrier. The reactants in the entrance channel can quantumly ‘feel’ this resonance state, which exists only in the exit channel.

We also calculated the reaction rate constants for the F + *ortho*-H$_2$ (o-H$_2$) reaction (solid red line in Fig. 5). The reaction rate constant of the o-H$_2$ reaction is only a few times smaller than that of the p-H$_2$ reaction, but much larger than that of the p-H$_2$ reaction without the ground resonance state. Because the energy of the ground resonance state is below the threshold energy of F + o-H$_2$(j = 1), the ground resonance state's contribution to the reaction is negligible in the low temperature regime. However, the excited resonance state should have a certain effect. We then investigated the effect of the first excited resonance state on the reaction rate constant for the F + o-H$_2$ reaction by taking out the resonance peaks of the excited resonance state in the reaction probabilities for all partial waves. Quite surprisingly, the rate constant without including the excited resonance is only ~30% smaller than that including the excited resonance state over the entire low temperature range. This implies that the effect of the excited resonance state on the reaction rate constants of the F + o-H$_2$(j = 1) reaction is dramatically differently from that of the ground state resonance on the reaction rate constants of the F + p-H$_2$(j = 0) reaction in the very low temperature regime (Fig. 5). Through dynamics analysis, we found that the difference is due to the fact that the non-resonance-induced tunnelling of the F + o-H$_2$(j = 1, k = 1) reaction through the reaction barrier in the low collision energy regime is already comparable to the resonance enhanced tunnelling in the F + o-H$_2$(j = 1, k = 0) reaction (Supplementary Fig. 9).

Because of the difference between the effect of resonances on the reaction rate constants of the F + p-H$_2$(j = 0) reaction and those of the F + o-H$_2$(j = 1) reaction, the effect of reaction resonances in the interstellar medium with different *ortho–para* ratios should also be quite different[47]. In Fig. 6, we show the results of calculations of the reaction rate constants for the F + n-H$_2$ reaction (*ortho–para* ratio of 3:1), and with *ortho* and *para* H$_2$ in the local thermal equilibrium condition in the low temperature instellar medium. The calculated reaction rate constants were compared with previously measured rate constants for the F + n-H$_2$ reaction[14]. The agreement is quite

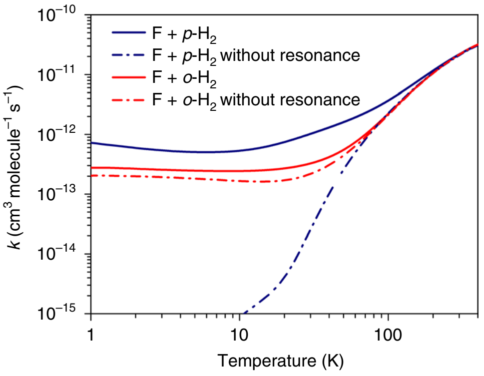

Fig. 5 | Calculated reaction rate constants. The calculated reaction rate constant, k, for the $F + p\text{-}H_2 \rightarrow HF + H$ and $F + o\text{-}H_2 \rightarrow HF + H$ reactions as a function of temperature. Solid lines represent the calculated reaction rate constants including the non-adiabatic spin–orbit effect based on the diabatic iCSZ-LWAL PESs. Dash-dotted lines are the calculated rate constants by excluding the contribution of related resonances for the two reactions.

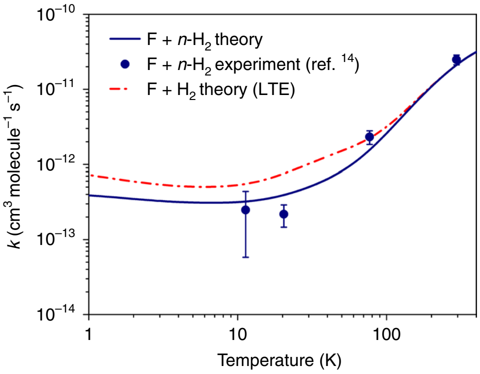

Fig. 6 | Calculated reaction rate constants. The calculated reaction rate constants k are shown for the $F + n\text{-}H_2 \rightarrow HF + H$ reaction (blue solid line) and the $F + H_2 \rightarrow HF + H$ reaction (red dash-dotted line) under the local thermal equilibrium (LTE) as a function of temperature. Filled circles are experimental results from ref. [14]. Lines represent the calculated rate constants including the non-adiabatic spin–orbit effect based on the diabatic iCSZ-LWAL PESs.

good, suggesting that the new diabatic PESs are not only accurate for reaction dynamics but also for low temperature kinetics. We also investigated the effect of the position of the reaction resonance state on the rate constant by shifting the resonance state energy up and down by 10% (~0.5 meV). The calculated reaction rate at 1 K for this reaction would change by ~35% with this resonance energy shift. Therefore, with the accurate resonance picture obtained in this work, the calculated reaction rate constants for the $F + H_2$ reaction presented in this work should be sufficiently accurate for modelling interstellar chemistry in the entire low temperature regime.

Conclusion

In this work, a unique type of quantum resonance-enhanced tunnelling effect in the $F + p\text{-}H_2 \rightarrow HF + H$ reaction has been characterized by a combined high-resolution crossed molecular beams experiment, a high-resolution negative ion photoelectron spectroscopy experiment and an accurate quantum reactive scattering theoretical study. The two state-of-the-art experimental results are in excellent agreement, and also agree with the theoretical calculations very well. It is found that this interesting tunnelling effect is fully responsible for the unusual chemical reactivity of $F + p\text{-}H_2$ in the low temperature interstellar medium, but has a much smaller effect on the chemical reactivity of $F + o\text{-}H_2$. Using the newly constructed diabatic iCSZ-LWAL PESs, accurate reaction rate constants for the $F + H_2$ reaction in the low temperature regime are calculated using a converged quantum reactive scattering method. These reaction rate constants should be sufficiently accurate for modelling interstellar chemistry. From the comparison between theory and experiment in this work, the iCSZ PES and iCSZ-LWAL PESs developed in this work are shown to be accurate PESs for describing the reaction resonance dynamics in the $F + H_2$ reaction.

Methods

Experiment. The H_2 beam was generated by expanding p-H_2 mixed with Ne through a modified general valve at a stagnation pressure of 20 psi. The pulsed valve for generating the H_2 beam was cooled to liquid nitrogen temperature. The velocity of the H_2 beam could be varied from 0.7 to 1.35 km s^{-1} with different mixing ratio of H_2 and Ne. The p-H_2 was made by passing normal H_2 gas through a ferromagnetic catalyst at ~20 K then stored in an aluminium tank at 500 psi at room temperature (the sample has a shelf life of ~10 days, with no significant conversion, as monitored by the thermal conductance method). The purity of the p-H_2 is better than 97%. The speed ratio of the H_2/Ne beam was determined to be between 20 and 35, which varies with different mixing ratios of the H_2/Ne sample. The F atom beam was produced by a double-stage pulse discharge of F_2 seeded in a mixture of He/Ne with varying mixing ratio at a stagnation pressure of 100 psi. The F atom beam was also cooled by liquid nitrogen to slow the beam velocity and to reduce the speed ratio to achieve better energy resolution for the experiment. The F atom beam velocity could be varied from 0.8 to 1.5 km s^{-1} with a speed ratio of ~20 using this method. By slowing both the F atom and H_2 beams using liquid-nitrogen-cooled pulsed valves and optimizing the rotating beam source design, a minimum crossing angle as low as 26° between the two beams was reached, allowing a reaction collision energy as low as 1.21 meV to be achieved. The energy spread of the collision energy was estimated to be ~10% of the collision energy.

Theory. A time-dependent wavepacket method for describing the coupled states' reactive scattering processes was applied in the quantum dynamics calculations to obtain the product quantum state-resolved S matrices, for which we only applied the reactant Jacobi coordinate during the wavepacket propagation. The fourth-order split operator was applied to propagate the wavepacket. The numerical parameters used in the calculations were capable of giving converged DCSs. For more details of the theory describing the dynamics of triatomic reactions, see refs. [42,43]. For the adiabatic reactive scattering model we used the ABC code, which uses the time-independent hyperspherical coordinate method, to calculate the product quantum state-resolved S matrices. The parameters for the ABC code adopted in this work are similar to those in our previous work[40].

Data availability

Data supporting the findings of this study are available from the corresponding authors on request.

Code availability

The accurate iCSZ and iCSZ-LWAL PESs developed in this work are available from the corresponding authors on request.

Received: 21 September 2018; Accepted: 7 May 2019;
Published online: 24 June 2019

References

1. Bell, R. P. *The Tunnel Effect in Chemistry* (Chapman & Hall, London, 1980).
2. Zuev, P. S. et al. Carbon tunnelling from a single quantum state. *Science* **299**, 867–870 (2003).
3. Fleming, G. R., Scholes, G. D. & Cheng, Y. C. Quantum effects in biology. *Procedia Chem.* **3**, 38–57 (2011).
4. Jankunas, J. & Osterwalder, A. Cold and controlled molecular beams: production and application. *Annu. Rev. Phys. Chem.* **66**, 241–262 (2015).
5. Kaiser, R. I., Parker, D. S. N. & Mebel, A. M. Reaction dynamics in astrochemistry: low-temperature pathways to polycyclic aromatic hydrocarbons in the interstellar medium. *Annu. Rev. Phys. Chem.* **66**, 43–67 (2015).
6. Wang, T. et al. Dynamical resonances in chemical reactions. *Chem. Soc. Rev.* **47**, 6744–6763 (2018).
7. Neufeld, D. A., Zmuidzinas, J., Schilke, P. & Phillips, T. G. Discovery of interstellar hydrogen fluoride. *Astrophys. J.* **488**, L141–L144 (1997).
8. Agundez, M. et al. HIFI detection of hydrogen fluoride in the carbon star envelope IRC+10216. *Astron. Astrophys.* **533**, L6 (2011).

9. Monje, R. R. et al. Herschel/HIFI observations of hydrogen fluoride toward Sagittarius B2(M). *Astrophys. J. Lett.* **734**, L23 (2011).
10. Indriolo, N., Neufeld, D. A., Seifahrt, A. & Richter, M. J. Direct determination of the HF/H_2 abundance ratio in interstellar gas. *Astrophys. J.* **764**, 188 (2013).
11. Berteloite, C. et al. Kinetics and dynamics of the $S(^1D_2)+H_2 \rightarrow SH+H$ reaction at very low temperatures and collision energies. *Phys. Rev. Lett.* **105**, 203201 (2010).
12. Lara, M. et al. Dynamics of the $S(^1D_2)+H_2$ reaction at collision energies approaching the cold regime: a stringent test for theory. *Phys. Rev. Lett.* **109**, 133201 (2012).
13. Lara, M. et al. Observation of partial wave structures in the integral cross section of the $S(^1D_2)+H_2(j=0)$ reaction. *Phys. Chem. Chem. Phys.* **13**, 8127–8130 (2011).
14. Tizniti, M. et al. The rate of the $F+H_2$ reaction at very low temperatures. *Nat. Chem.* **6**, 141–145 (2014).
15. Schatz, G. C. Detecting resonance. *Science* **288**, 1599–1600 (2000).
16. Fernandez-Alonso, F. & Zare, R. N. Scattering resonances in the simplest chemical reaction. *Annu. Rev. Phys. Chem.* **53**, 67–99 (2002).
17. Liu, K. Crossed-beam studies of neutral reactions: state-specific differential cross sections. *Annu. Rev. Phys. Chem.* **52**, 139–164 (2001).
18. Liu, K. Quantum dynamical resonances in chemical reactions: from A+BC to polyatomic systems. *Adv. Chem. Phys.* **149**, 1–46 (2012).
19. Yang, X. M. & Zhang, D. H. Dynamics resonances in the fluorine atom reaction with the hydrogen molecule. *Acc. Chem. Res.* **41**, 981–989 (2008).
20. Schatz, G. C., Bowman, J. M. & Kuppermann, A. Large quantum effects in the collinear $F+H_2 \rightarrow HF+H$ reaction. *J. Chem. Phys.* **58**, 4023–4025 (1973).
21. Wu, S.-F., Johnson, B. R. & Levine, R. D. Quantum mechanical computational studies of chemical reactions: III. Collinear A+BC reaction with some model potential energy surfaces. *Mol. Phys.* **25**, 839–856 (1973).
22. Neumark, D. M. et al. Molecular beam studies of the $F+D_2$ and F+HD reactions. *J. Chem. Phys.* **82**, 3067–3077 (1985).
23. Neumark, D. M., Wodtke, A. M., Robinson, G. N., Hayden, C. C. & Lee, Y. T. Molecular beam studies of the $F+H_2$ reaction. *J. Chem. Phys.* **82**, 3045–3066 (1985).
24. Aoiz, F. J. et al. Classical dynamics for the $F+H_2 \rightarrow HF+H$ reaction on a new ab initio potential energy surface: a direct comparison with experiment. *Chem. Phys. Lett.* **223**, 215–226 (1994).
25. Castillo, J. F., Manolopoulos, D. E., Stark, K. & Werner, H. J. Quantum mechanical angular distributions for the $F+H_2$ reaction. *J. Chem. Phys.* **104**, 6531–6546 (1996).
26. Stark, K. & Werner, H. J. An accurate multireference configuration interaction calculation of the potential energy surface for the $F+H_2 \rightarrow HF+H$ reaction. *J. Chem. Phys.* **104**, 6515–6530 (1996).
27. Ren, Z. et al. Probing the resonance potential in the F atom reaction with hydrogen deuteride with spectroscopic accuracy. *Proc. Natl Acad. Sci. USA* **105**, 12662–12666 (2008).
28. Skodje, R. T. et al. Resonance mediated chemical reaction: $F+HD \rightarrow HF+D$. *Phys. Rev. Lett.* **85**, 1206 (2000).
29. Dong, W. R. et al. Transition state spectroscopy of partial wave resonances in the F+HD reaction. *Science* **327**, 1501–1502 (2010).
30. Manolopoulos, D. E. et al. The transition state of the $F+H_2$ reaction. *Science* **262**, 1852–1855 (1993).
31. Kim, J. B. et al. Spectroscopic observation of resonances in the $F+H_2$ reaction. *Science* **349**, 510–513 (2015).
32. Qiu, M. H. et al. Observation of Feshbach resonances in the $F+H_2 \rightarrow HF+H$ reaction. *Science* **311**, 1440 (2006).
33. Wang, X. A. et al. HF($v'=3$) forward scattering in the $F+H_2$ reaction: shape resonance and slow-down mechanism. *Proc. Natl Acad. Sci. USA* **105**, 6227–6231 (2008).
34. Qiu, M. H. et al. High resolution time-of-flight spectrometer for crossed molecular beam study of elementary chemical reactions. *Rev. Sci. Instrum.* **76**, 083107 (2005).
35. Wang, T. et al. Dynamical resonances accessible only by reagent vibrational excitation in the $F+HD \rightarrow HF+D$ reaction. *Science* **342**, 1499–1502 (2013).
36. Yang, T. G. et al. Extremely short-lived reaction resonances in $Cl+HD(v=1) \rightarrow DCl+H$ due to chemical bond softening. *Science* **347**, 60–63 (2015).
37. Neumark, D. M. Probing the transition state with negative ion photodetachment: experiment and theory. *Phys. Chem. Chem. Phys.* **7**, 433–442 (2005).
38. Yu, D., Chen, J., Cong, S. L. & Sun, Z. Theoretical study of FH_2^- electron photodetachment spectra on new ab initio potential energy surfaces. *J. Phys. Chem. A* **119**, 12193–12208 (2015).
39. Blondel, C., Delsart, C. & Goldfarb, F. Electron spectrometry at the μeV level and the electron affinities of Si and F. *J. Phys. At. Mol. Opt. Phys.* **34**, L281–L288 (2001).
40. Chen, J., Sun, Z. & Zhang, D. H. An accurate potential energy surface for the $F+H_2 \rightarrow HF+H$ reaction by the coupled-cluster method. *J. Chem. Phys.* **142**, 024303 (2015).
41. Skouteris, D., Castillo, J. F. & Manolopoulos, D. E. ABC: a quantum reactive scattering program. *Comput. Phys. Commun.* **133**, 128–135 (2000).
42. Sun, Z., Zhang, D. H. & Alexander, M. H. Time-dependent wavepacket investigation of state-to-state reactive scattering of Cl with *para*-H_2 including the open-shell character of the Cl atom. *J. Chem. Phys.* **132**, 034308 (2000).
43. Sun, Z., Yang, W. T. & Zhang, D. H. Higher-order split operator schemes for solving the Schrödinger equation in the time-dependent wave packet method: applications to triatomic reactive scattering calculations. *Phys. Chem. Chem. Phys.* **14**, 1827–1845 (2012).
44. Lique, F., Li, G. L., Werner, H.-J. & Alexander, M. H. Non-adiabatic coupling and resonances in the $F+H_2$ reaction at low energies. *J. Chem. Phys.* **134**, 231101 (2011).
45. Alexander, M. H., Manolopoulos, D. & Werner, H.-J. An investigation of the $F+H_2$ reaction based on a full ab initio description of the open-shell character of the $F(^2P)$ atom. *J. Chem. Phys.* **113**, 11084 (2000).
46. Weichman, M. L. et al. Feshbach resonances in the exit channel of the $F+CH_3OH \rightarrow HF+CH_3O$ reaction observed using transition-state spectroscopy. *Nat. Chem.* **9**, 950–955 (2017).
47. Sternberg, A. & Neufeld, D. The ratio of *ortho*- to *para*-H_2 in photodissociation regions. *Astrophys. J.* **516**, 371–380 (1999).

Acknowledgements

C.X., Z.S., D.H.Z. and X.Y. acknowledge financial support for this research from the National Science Foundation of China (grants 21688102, 21590800, 21127902 and 21433009) and the Chinese Academy of Sciences (grants XDB 17010000). D.M.N. thanks the Air Force Office of Scientific Research for funding this research under grant no. FA9550-16-1-0097. M.H.A. thanks the US National Science Foundation for support under grant no. CHE-1565872.

Author contributions

X.Y., D.H.Z., Z.S., C.X., D.M.N. and M.H.A. conceived and supervised the research. The experiments were carried out by T.Y., L.H., T.W., D.D. and C.X. Data analysis and interpretation were performed by T.Y., L.H., T.W., D.D., C.X. and X.Y. Theoretical calculations were performed by Z.S., J.C., F.L., M.H.A. and D.H.Z. The manuscript was written by X.Y., Z.S., M.H.A., D.Z. and D.M.N., with contributions from all authors. All authors contributed to discussions about the content of the paper.

Competing interests

The authors declare no competing interests.

Additional information

Supplementary information is available for this paper at https://doi.org/10.1038/s41557-019-0280-3.

Reprints and permissions information is available at www.nature.com/reprints.

Correspondence and requests for materials should be addressed to M.H.A., Z.S., X.Y. or D.M.N.

Publisher's note: Springer Nature remains neutral with regard to jurisdictional claims in published maps and institutional affiliations.

© The Author(s), under exclusive licence to Springer Nature Limited 2019